Chapter 5 Part 6: Highlights

1. **Requirement High Re: $p = \frac{5}{3}$ only achieved very large R_λ >> laboratory flows.**

$$E(\kappa) \sim \kappa^{-p} \quad p = \frac{5}{3} - 8R_\lambda^{-3/4}$$

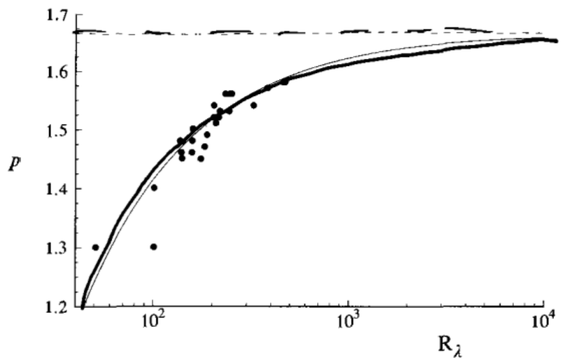

Fig. 6.29. The spectrum power-law exponent p ($E(\kappa) \sim \kappa^{-p}$) as a function of the Reynolds number in grid turbulence: symbols, experimental data of Mydlarski and Warhaft (1998); dashed line, $p = \frac{5}{3}$; solid line, empirical curve $p = \frac{5}{3} - 8R_\lambda^{-3/4}$.

Energy cascade not one way and involves multiple size eddies with net transfer toward smaller scales. In wave number space, as per Fourier series NS, involves triads of wave numbers with two nearly equal and third much smaller.

2. **Higher-order statistics**

Simplest examples of higher-order statistics are the normalized velocity-derivative moments:

$$M_n = \overline{(u_{1,1})^n} / \overline{(u_{1,1})^2}^{\,n/2}$$

For $n = 3$ and $n = 4$, these are the velocity-derivative skewness S and kurtosis K.

$$M_3 = \overline{(u_{1,1})^3} / \overline{(u_{1,1})^2}^{\,3/2} \quad = \quad \text{Skewness } (S = 0 \text{ for}$$

$S < 0 = f($ vortex stretching and related energy transfer between scales) and measure of the bias or asymmetry in the velocity fluctuations between + and – values.

$$M_4 = \overline{(u_{1,1})^4} / \overline{(u_{1,1})^2}^{\,2} \;=\; \text{Kurtosis } (K = 3 \text{ for Gaussian})$$

Measure of how much the velocity fluctuations are congregated at large and small values.

Kolmogorov originally assumed, the PDF of the velocity fluctuations is homogeneous and isotropic, which is often approximated as Gaussian, such that for each n, M_n is a constant; however, in fact, S and K are not constant but increase with Re.

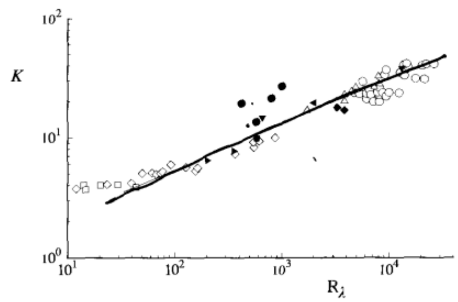

Fig. 6.30. Measurements (symbols) compiled by Van Atta and Antonia (1980) of the velocity-derivative kurtosis as a function of Reynolds number. The solid line is $K \sim R_\lambda^{3/8}$.

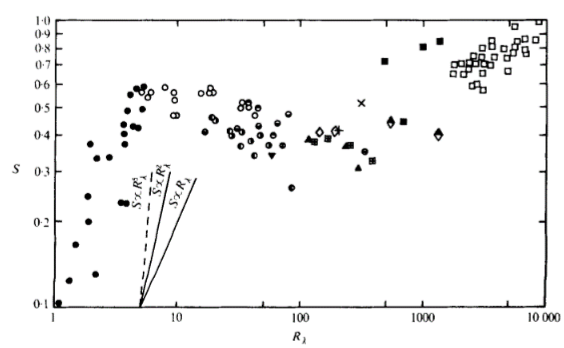

FIGURE 1. Measurements of the velocity-derivative skewness in various turbulent flows plotted *vs.* the turbulent Reynolds number (see table 1 for symbols).

Type of flow	Author(s)	Symbol
Nearly isotropic grid turbulence	Batchelor & Townsend (1949)	◑
	Stewart & Townsend (1951)	◐
	Mills *et al.* (1958)	◒
	Frenkiel & Klebanoff (1971)	◓
	Kuo & Corrsin (1971)	⊕
	Betchov & Lorenzen (1974)	⊖
	Bennett & Corrsin (1978)	○
	Present data	●
Homogeneous shear flow	Tavoularis (1978)	◇
Duct flow	Comte-Bellot (1965)	▲
	Elena, Chauve & Dumas (1977)	▼
Mixing layers	Wyngaard & Tennekes (1970)	+
	Champagne, Pao & Wygnanski (1976)	×
Axisymmetric jet	Friehe, Van Atta & Gibson (1972)	⬘
	New measurements	⬙
Boundary layer	Ueda & Hinze (1975)	⊞
Atmosphere	Gibson, Stegen & Williams (1970)	■
	Wyngaard & Tennekes (1970)	□

TABLE 1

Higher order statistics pertaining to the inertial subrange are provided by the longitudinal velocity structure functions (Chapter 4 Part 8):

$$D_n(r) \equiv \overline{(\Delta_r u)^n}$$

$$\Delta_r u \equiv U_1(\underline{x} + \widehat{e_1} r, t) - U_1(\underline{x}, t)$$

Recall for the second (Chapter 4, Part 8) and third (Part 3, pg. 18) order structure functions $D_2(r), D_3(r)$ in the inertial sub-range:

$$D_2 = D_{LL}(r,t) = C_2(\varepsilon r)^{2/3}$$

$$D_3 = D_{LLL}(r,t) = C_3 \varepsilon r$$

Which were determined according to Kolmogorov's second hypothesis, for $L \gg r \gg \eta$, $D_n(r)$ based on the assumption that they depend only on ε and r, i.e.,

$$D_n(r) \equiv \overline{(\Delta_r u)^n} = C_n(\varepsilon r)^{n/3}$$

Where C_n are constants ($C_2 = 2, C_3 = -4/5$).

More generally in the inertial subrange,

$$D_n(r) \sim r^{\zeta_n}$$

But the measured exponents differ from the Kolmogorov prediction, i.e., $\zeta_n = \frac{n}{3}$, as clearly $\zeta_n \neq \frac{n}{3}$ for n ≥ 4.

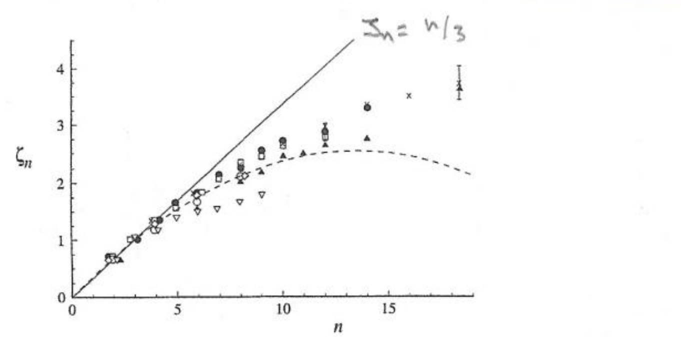

Fig. 6.31. Measurements (symbols) compiled by Anselmet *et al.* (1984) of the longitudinal velocity structure function exponent ζ_n in the inertial subrange, $D_n(r) \sim r^{\zeta_n}$. The solid line is the Kolmogorov (1941) prediction, $\zeta_n = \frac{1}{3}n$; the dashed line is the prediction of the refined similarity hypothesis, Eq. (6.323) with $\mu = 0.25$.

It is instructive to examine the PDFs that underlie M_n. For example, for n=1, the PDF is denoted by $f_Z(z)$, where Z is the standardized derivative

$$Z \equiv u_{1,1} / \overline{\left(u_{1,1}\right)^2}^{1/2}$$

$$\boxed{M_n \equiv 2 \int_0^\infty z^n f_Z(z) dz}$$

$$\boxed{M_1 = \overline{\left(u_{1,1}\right)^1} / \overline{\left(u_{1,1}\right)^2}^{1/2}}$$

Appendix

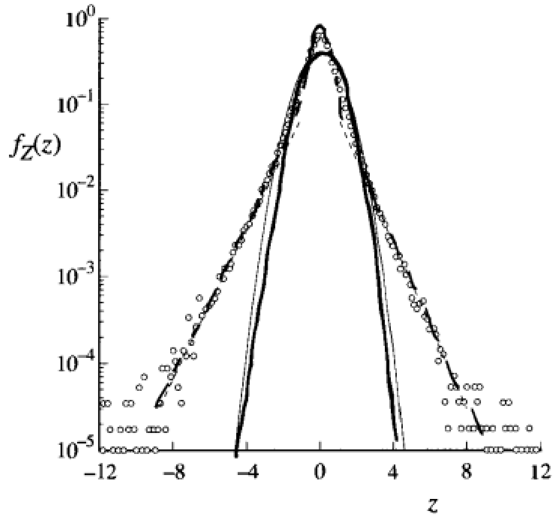

Fig. 6.32. The PDF $f_Z(z)$ of the normalized velocity derivative $Z \equiv (\partial u_1/\partial x_1)/\langle(\partial u_1/\partial x_1)^2\rangle^{1/2}$ measured by Van Atta and Chen (1970) in the atmospheric boundary layer (high Re). The solid line is a Gaussian; the dashed lines correspond to exponential tails (Eqs. (6.309) and (6.310)).

low probability tails can make vast contributions to higher moments. For example, compare the tails for

$$M_n^{(5)} \equiv 2 \int_5^\infty z^n f_Z(z) dz$$

Using (0) and considering only even moments so we can compare with Gaussian values.

Table 6.3. *Contributions $M_n^{(5)}$ from the exponential tails ($|Z| > 5$) of the PDF of Z to the moments M_n according to Eqs. (6.310) and (6.311)*

Moment n	Tail contribution $M_n^{(5)}$	Gaussian value M_n
0	0.003	1
2	0.1	1
4	4.2	3
6	220	15
8	1.5×10^4	105
10	1.4×10^6	945

The super skewness $M_6 = 220$, while Gaussian value is 15.

3. **Dissipation intermittency**

Discrepancies between M_n and $D_n(r)$ with EFD are attributed to the phenomenon of *internal intermittency* and accounted for in the *refined similarity hypotheses*, which introduces several new quantities related to dissipation.

One-dimensional surrogates for instantaneous dissipation and average of ε_0 within a sphere $\forall(r)$ of radius r are represented by:

$$\hat{\varepsilon}_0 = 15\nu\left(\frac{\partial u_1}{\partial x_1}\right)^2 \quad (2A) \quad \tilde{\varepsilon} = 15\nu\overline{\left(\frac{\partial u_1}{\partial x_1}\right)^2}$$

$$\hat{\varepsilon}_r(x,t) = \frac{1}{r}\int_0^r \hat{\varepsilon}_r(x+r,t)\,dr$$

And in locally isotropic turbulence, each of these quantities have mean ε,

i.e., $\langle\hat{\varepsilon}_0\rangle = \langle\hat{\varepsilon}_r(\underline{x},t)\rangle = \varepsilon = \tilde{\varepsilon}\ (2B)$.

$\hat{\varepsilon}_0$ intermittently attains high values.

R_λ laboratory (moderate) → $\hat{\varepsilon}_0/\ \varepsilon \approx 15$

R_λ atmosphere (high) → $\hat{\varepsilon}_0/\ \varepsilon \approx 50$

Kolmogorov conjectured that:

$$\frac{\overline{\hat{\varepsilon}_0{}^2}}{\varepsilon^2} \sim (L/\eta)^\mu$$

$$\frac{\overline{\hat{\varepsilon}_r{}^2}}{\varepsilon^2} \sim (L/r)^\mu$$

Where $L = k^{3/2}/\varepsilon$. For the inertial subrange, i.e., $\eta \ll r \ll L$ and $\mu > 0$ = constant=intermittency exponent. Note above equations are for mean square $\hat{\varepsilon}_0$ and $\hat{\varepsilon}_r$.

EFD for $\frac{\overline{\hat{\varepsilon}_r{}^2}}{\varepsilon^2}$ shows $\mu = 0.25 \pm 0.05$.

Refined similarity hypotheses

Original first hypothesis: $\Delta_r u$ for $r \ll L$ are universal and $f(\varepsilon, \nu)$.

Refined first hypothesis: $\Delta_r u$ for $r \ll L$ are universal and $f(\varepsilon_r, \nu)$.

Refined second hypothesis: $\Delta_r u$ for $\eta \ll r \ll L$ are universal and $f(\varepsilon_r)$.

The structure functions in the inertial subrange are:

$$D_n(r) = \langle(\Delta_r u)^n\rangle = \langle C_n(\varepsilon r)^{n/3}|_{\varepsilon=\varepsilon_r}\rangle = C_n\langle {\varepsilon_r}^{n/3}\rangle r^{n/3}$$

Where C_n are universal constants and ε_r is a volume averaged variable, as per $\hat{\varepsilon}_r(x,t)$.

For $n = 3$, since $\overline{\varepsilon_r} = \varepsilon$, the original and the refined hypotheses make the same prediction, i.e., $C_3 = -4/5$, which represents the Kolmogorov 4/5 law.

For other n, $\overline{{\varepsilon_r}^{n/3}}$ can be determined from the PDF of ε_r, which is assumed to be log-normally distributed, i.e., $\ln(\varepsilon_r/\varepsilon_{ref})$ has Gaussian distribution such that:

$$\frac{\overline{{\varepsilon_r}^n}}{\overline{\varepsilon_r}^n} \sim (L/r)^{n(n-1)\mu/2} \qquad (3)$$

Pope Ex 6.37
Appendix A.3

Consequently, if the structure function is predicted to scale as $D_n(r) \sim r^{\zeta_n}$,

$$D_n(r) = C_n \langle {\varepsilon_r}^{\frac{n}{3}}\rangle r^{\frac{n}{3}}$$

$$= C_n \overline{\varepsilon_r}^{n/3} L^{n(n-1)\mu/6} r^{\overbrace{n/3 - n(n/3-1)\mu/6}^{\boxed{\zeta_n}}}$$

$$\zeta_n = \frac{1}{3}n\left[1 - \frac{1}{6}\mu(n-3)\right]$$

For $n \leq 10$, this prediction is in reasonable agreement with Fig. 6.31. For large n, the large errors are due to the assumption of the log-normal distribution.

For $D_2(r)$:

$$\zeta_2 = \frac{2}{3} + \frac{1}{9}\mu \approx \frac{2}{3} + \frac{1}{36}$$

Applying a Fourier transform to $D_n(r)$ $\boxed{\text{Appendix A.4}}$ results in an expression for the energy spectrum in the inertial range of the form:

$$E(k) = A\overline{\varepsilon_r}^{\frac{n}{3}} k^{-\frac{5}{3}} (Lk)^{-\mu}$$

This shows that in the inertial-range the spectrum is predicted to be a power law $E(\kappa) \sim \kappa^{-p}$ with

$$p = \frac{5}{3} + \frac{1}{9}\mu \approx \frac{5}{3} + \frac{1}{36}$$

Hence, only small correction to the -5/3 spectrum.

$$M_n = \frac{\overline{(u_{1,1})^n}}{\overline{(u_{1,1})^2}^{n/2}} = \frac{\overline{C_n}\left(\frac{\overline{\varepsilon_r}}{\nu}\right)^{\frac{n}{2}}}{\left(\overline{C_2}\left(\frac{\overline{\varepsilon_r}}{\nu}\right)\right)^{n/2}} = \frac{\overline{C_n}\,\overline{\varepsilon_r^{n/2}}}{\left(\overline{C_2}\,\overline{\varepsilon_r}\right)^{n/2}} \qquad (4)$$

$$M_3 = \frac{\overline{C_n}\,\overline{\varepsilon_r^{3/2}}}{\left(\overline{C_2}\,\overline{\varepsilon_r}\right)^{3/2}} = \frac{\overline{C_n}}{\left(\overline{C_2}\right)^{3/2}}(L/r)^{3/2(3/2-1)\mu/2} = \frac{\overline{C_n}}{\left(\overline{C_2}\right)^{3/2}}(L/r)^{3\mu/8}$$

$$M_4 = \frac{\overline{C_n}\,\overline{\varepsilon_r^{4/2}}}{\left(\overline{C_2}\,\overline{\varepsilon_r}\right)^{4/2}} = \frac{\overline{C_n}}{\left(\overline{C_2}\right)^{3/2}}(L/r)^{2(2-1)\mu/2} = \frac{\overline{C_n}}{\left(\overline{C_2}\right)^{3/2}}(L/r)^{\mu}$$

$$-S \sim (L/r)^{3\mu/8}$$

$$K \sim (L/r)^{\mu}$$

$$-S \sim K^{3/8}$$

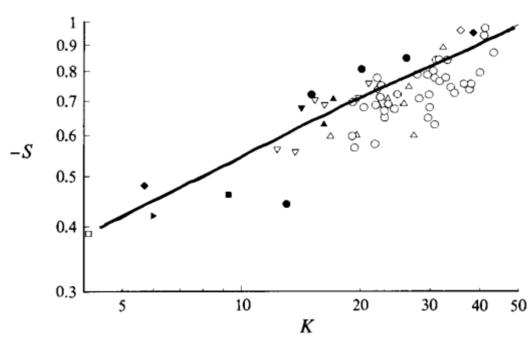

Fig. 6.33. Measurements of the velocity-derivative skewness S and kurtosis K compiled by Van Atta and Antonia (1980). The line is $-S \sim K^{3/8}$.